SUPPLEMENTARY INFORMATION

Scalable Fabrication of an Array-Type Fixed-Target Device for Automated Room Temperature X-ray Protein Crystallography

Sarthak Saha,[1] Yaozu Chen,[1] Silvia Russi,[2] Darya Marchany-Rivera,[2]
Aina Cohen,[2] Sarah L. Perry[1*]

[1] Department of Chemical Engineering, University of Massachusetts Amherst, MA, 01003, USA
[2] SLAC National Accelerator Laboratory, Menlo Park, California, 94025, USA

Correspondence email: perrys@engin.umass.edu

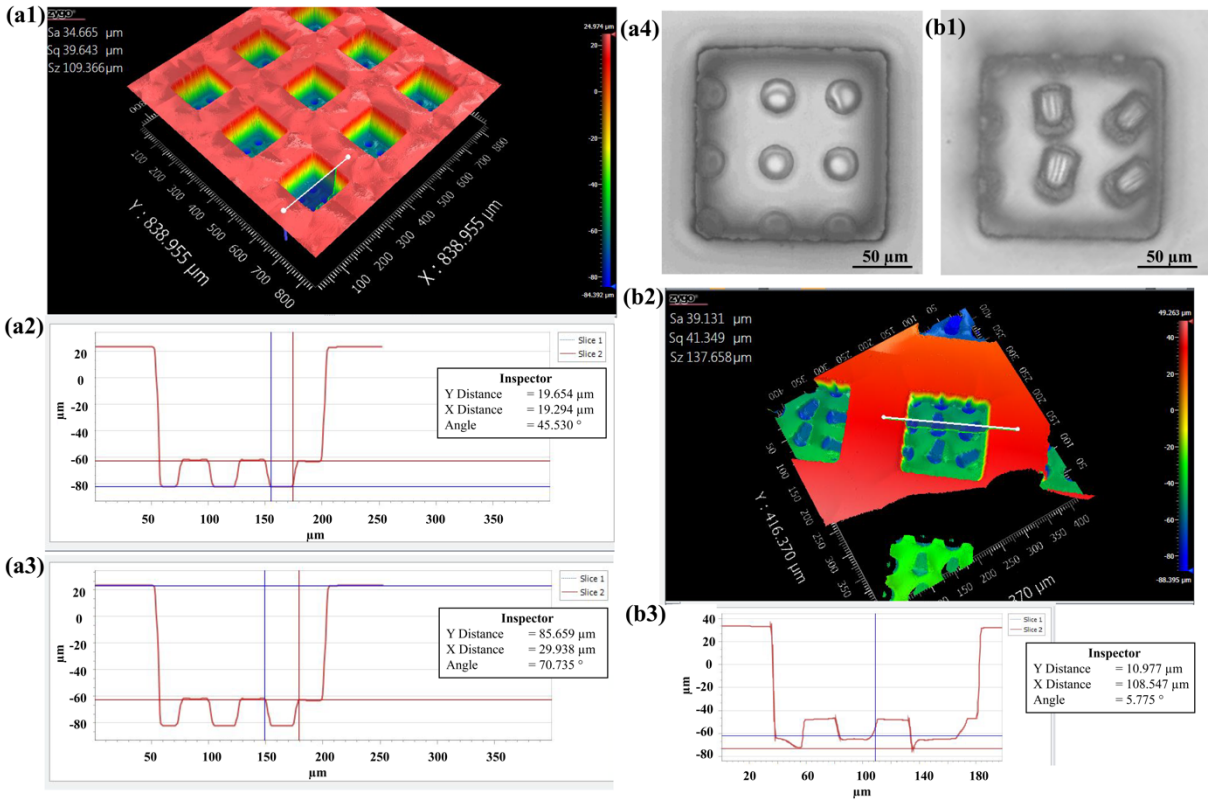

Figure S1. (a1) 3-D profilometry image of the NOA grids fabricated by R2R processing **(a2-a3)** 2-D cross sectional section of a single grid. **(a4)** Optical micrograph of a single grid fabricated using no added pressure. **(b1)** Optical micrograph of polymer grid fabricated using higher pressure showing deformations. **(b2-b3)** 3-D and 2-D profilometry image of the deformed NOA chip.

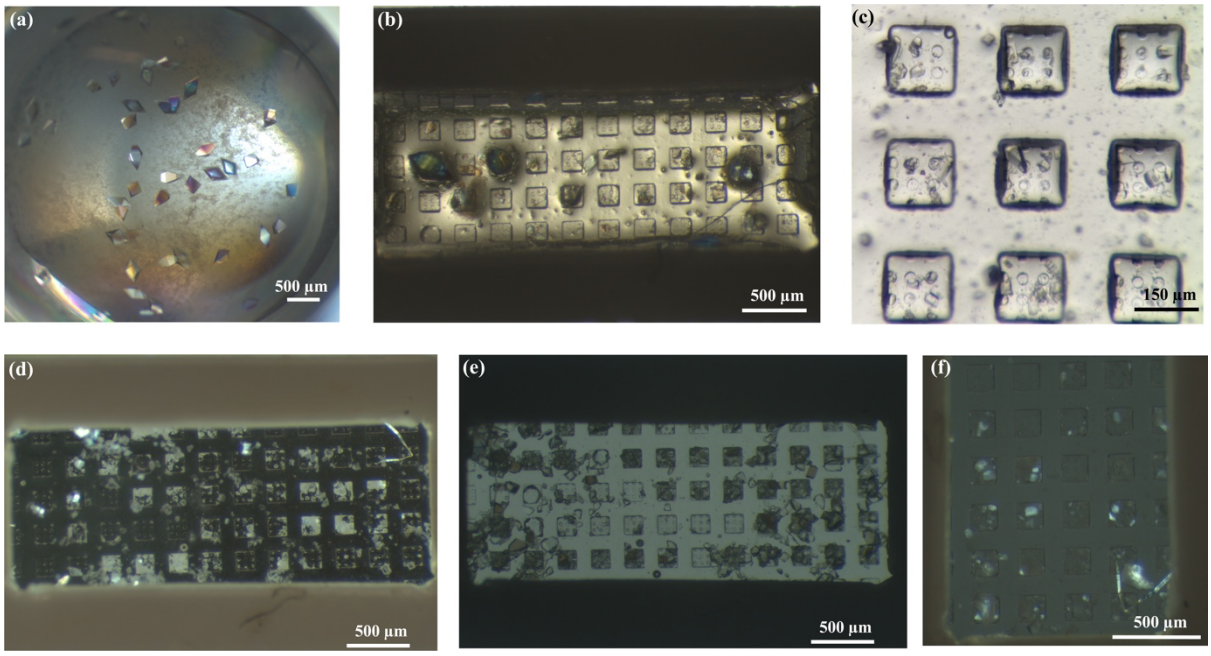

Figure S2. Polarized light microscopy images of (a) thaumatin crystals grown via sitting drop and (b) transferred into the AFD-X chip. Polarized light microscopy of (c-f) lysozyme crystals transferred into AFD-X at different crystal concentration.

Figure S3. (a) Photograph of AFD-X chips loaded with protein crystals inside the SSRL crystallization plate for safe transport. **(b)** Multiple loaded plates stacked into the thermal shipper box. **(c)** Overview image of the thermal shipper box containing the SSRL plates.

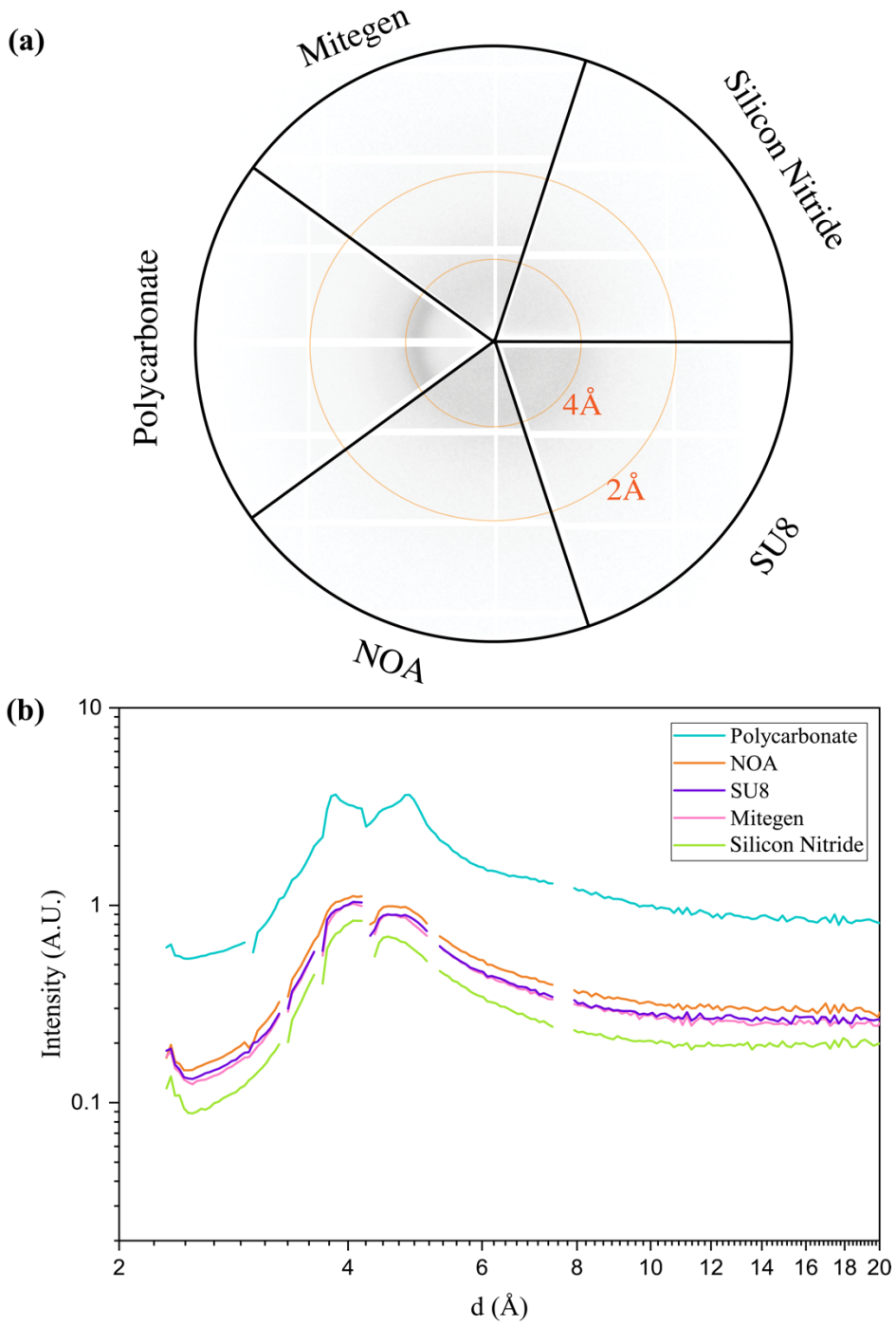

Figure S4. (a) The 2-D diffraction signal comparing the commercially available fixed-target devices made with 50 nm-thick silicon nitride,[1] 20 µm Mitegen Micromeshes, polycarbonate chips (~200 µm-thick),[2] and AFD-X developed using 20 µm NOA and SU-8. **(b)** Graph of the 1-D integrated X-ray intensity profiles comparing the relative strength of the observed diffraction signal from the materials shown in **(a)** alongside the AFD-X fabricated with SU-8. Data were collected at SSRL beamline 12-1.

S1. X-ray Crystallography and Crystal Isomorphism

We analyzed the statistical variation of the unit cell parameters for lysozyme, thaumatin and proteinase K crystals. After indexing and geometrical refinement of each crystal, the analysis was performed using methods described by Q. Liu *et al.*[3,4] A standard Euclidean distance, $\Delta_{j,k}$ was used to calculate the variation in crystal unit cell parameter. The Euclidean distance is a normalized distance using the unit cell parameter a, b, c, α, β, and γ of crystal *j* and *k* across *N* different crystals. It is normalized using the variance of these parameters over the population.

$$\Delta_{j,k} = \left[\frac{1}{\sigma^2}\sum_{u=\mathrm{a,b,c,\alpha,\beta,\gamma}}(u_j - u_k)^2\right]^{\frac{1}{2}} \quad \text{(S1)}$$

$$\sigma^2 = \left[\frac{1}{N}\sum_{k=1}^{N}(u_k - \bar{u}_k)^2\right] \quad \text{(S2)}$$

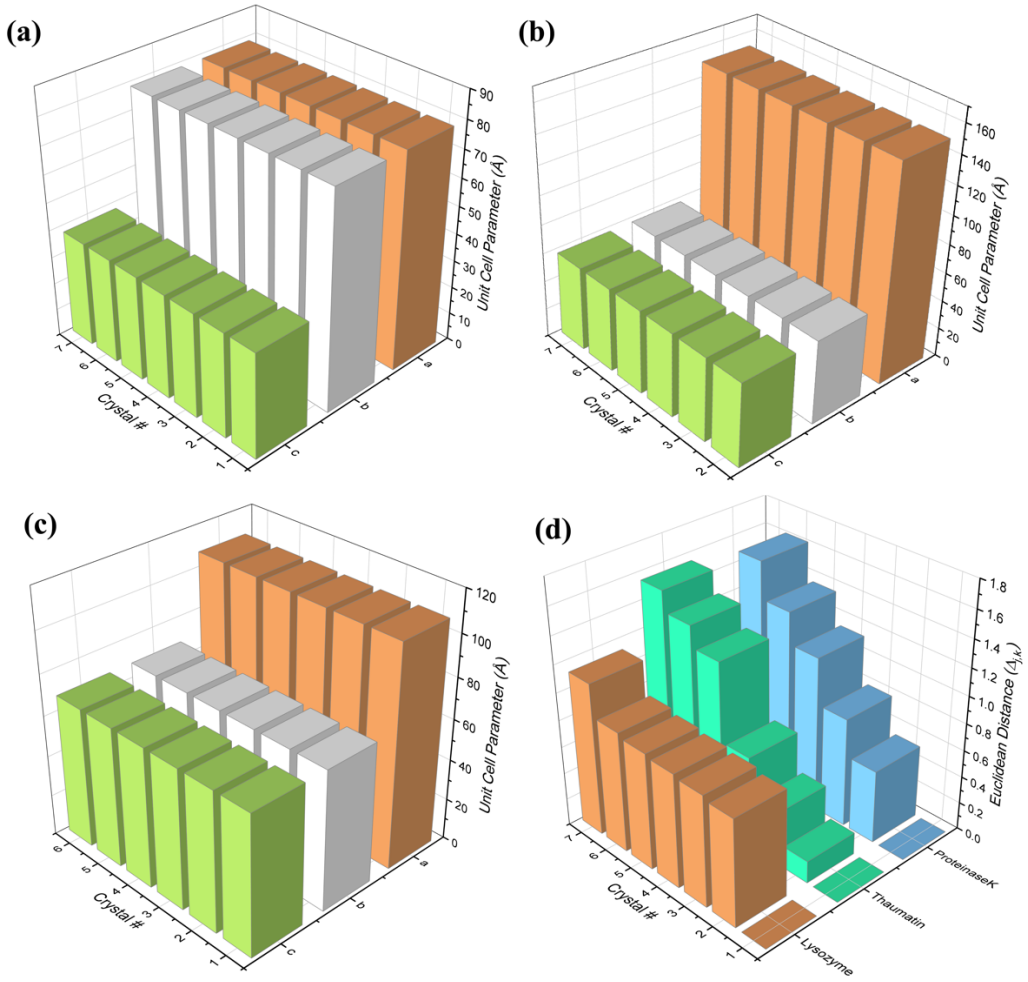

Figure S5. (a)-(c) Plots of the variation in the corresponding unit cell parameter across the 7 crystals of lysozyme, thaumatin each and 6 crystals of proteinase K analyzed. The data are available in Tables S1-S3, below. **(d)** Plot of the standard Euclidian distance $\Delta_{j,k}$ vs. crystal, showing the variation in the unit cell parameters of the three different protein crystals.

Table S1. Unit cell parameters for data collected across multiple lysozyme crystals.

Lysozyme	Unit Cell Parameter (Å)		
	a	**b**	**b**
Crystal 1	78.89	78.89	38.4
Crystal 2	78.89	78.89	38.31
Crystal 3	79.00	79.00	38.27
Crystal 4	78.96	78.96	38.26
Crystal 5	79.01	78.98	38.29
Crystal 6	78.80	78.81	38.34
Crystal 7	78.98	78.97	38.29

Table S2. Unit cell parameters for data collected across multiple thaumatin crystals.

Thaumatin	Unit Cell Parameter (Å)		
	a	**b**	**b**
Crystal 1	58.56	58.56	151.69
Crystal 2	58.52	58.52	151.66
Crystal 3	58.55	58.55	151.73
Crystal 4	58.54	58.55	151.72
Crystal 5	58.57	58.60	151.81
Crystal 6	58.54	58.54	151.77
Crystal 7	58.56	58.58	151.81

Table S3. Unit cell parameters for data collected across multiple proteinase K crystals

ProteinaseK	Unit Cell Parameter (Å)		
	a	**b**	**b**
Crystal 1	68.42	68.43	108.16
Crystal 2	68.41	68.43	108.13
Crystal 3	68.40	68.40	108.10
Crystal 4	68.44	68.45	108.13
Crystal 5	68.42	68.42	108.08
Crystal 6	68.42	68.42	108.07

References

1. Hunter, M. S. *et al.* Fixed-target protein serial microcrystallography with an X-ray free electron laser. *Sci Rep* **4**, 6026 (2014).
2. Baxter, E. L. *et al.* High-density grids for efficient data collection from multiple crystals. *Acta Crystallogr D Struct Biol* **72**, 2–11 (2016).
3. Liu, Q. & Hendrickson, W. A. Robust structural analysis of native biological macromolecules from multi-crystal anomalous diffraction data. *Acta Crystallogr D Biol Crystallogr* **69**, 1314–1332 (2013).
4. Liu, Q. *et al.* Structures from anomalous diffraction of native biological macromolecules. *Science* **336**, 1033–1037 (2012).